Electronic Supplementary Material (ESI) for Journal of Materials Chemistry A.
This journal is © The Royal Society of Chemistry 2017

Oxygen-Induced Defects at the Lead Halide Perovskite/Graphene Oxide Interfaces

Muge Acik,[a,*] In Kee Park,[b] Rachel E. Koritala,[a] Geunsik Lee,[b] Richard A. Rosenberg[c]

[a]Center for Nanoscale Materials, Argonne National Laboratory, Lemont, IL 60439

[b]Department of Chemistry, Ulsan National Institute of Science and Technology, Ulsan, Korea 689-798

[c]Advanced Photon Source, X-ray Science Division, Argonne National Laboratory, Lemont, IL 60439

*Corresponding Author: macik@anl.gov

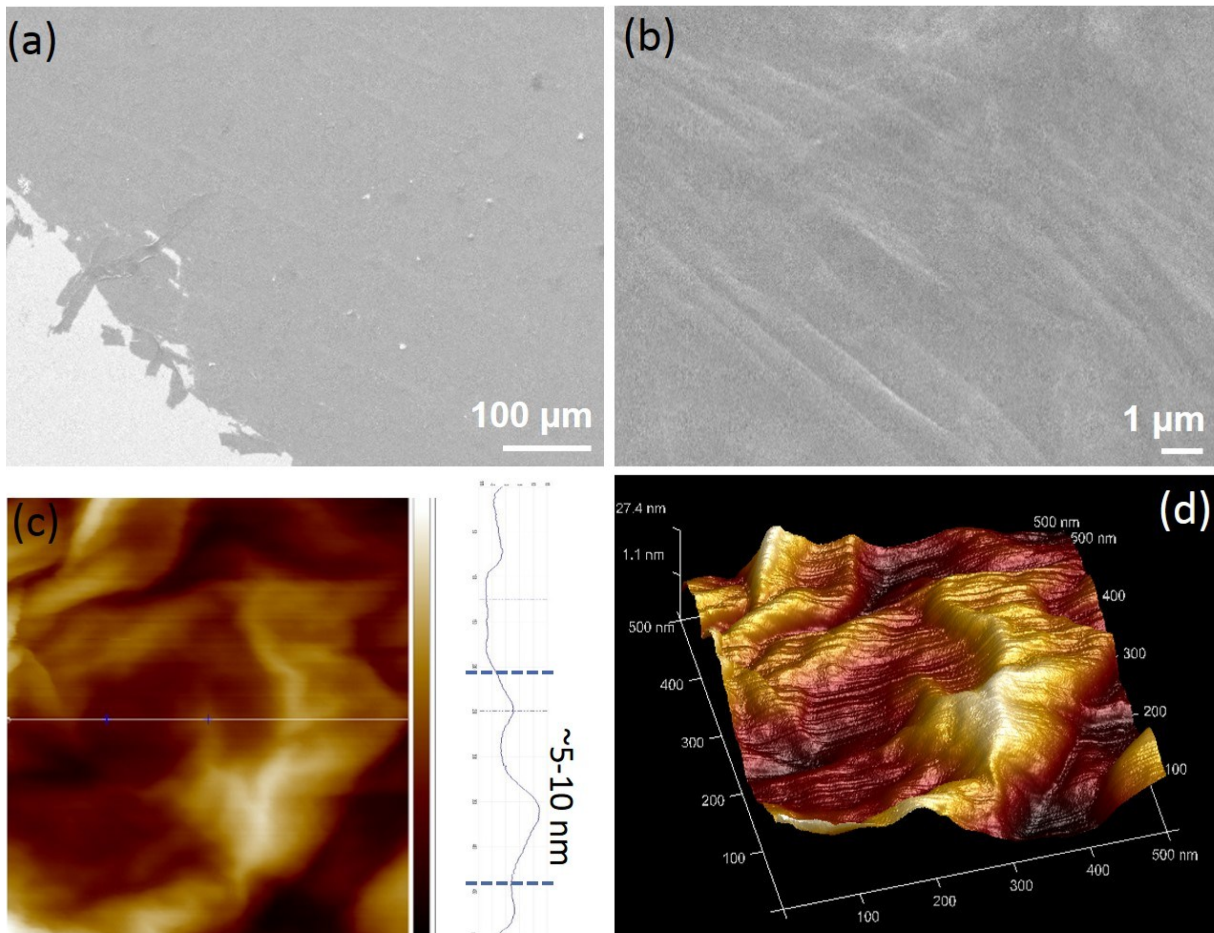

Figure S1. a) Top-down SEM image of a continuous GO (3-5 layers) thin film with natural wrinkles and ripples as shown with a high magnification image in (b). The scale bars represent 100 μm and 1 μm in (a)-(b), respectively. c) AFM image of a GO (3-5 L) with a thickness of 5-10 nm, and an average surface roughness of R_{max}~20 nm shown with a 3D topography (500x500 nm) in (d).

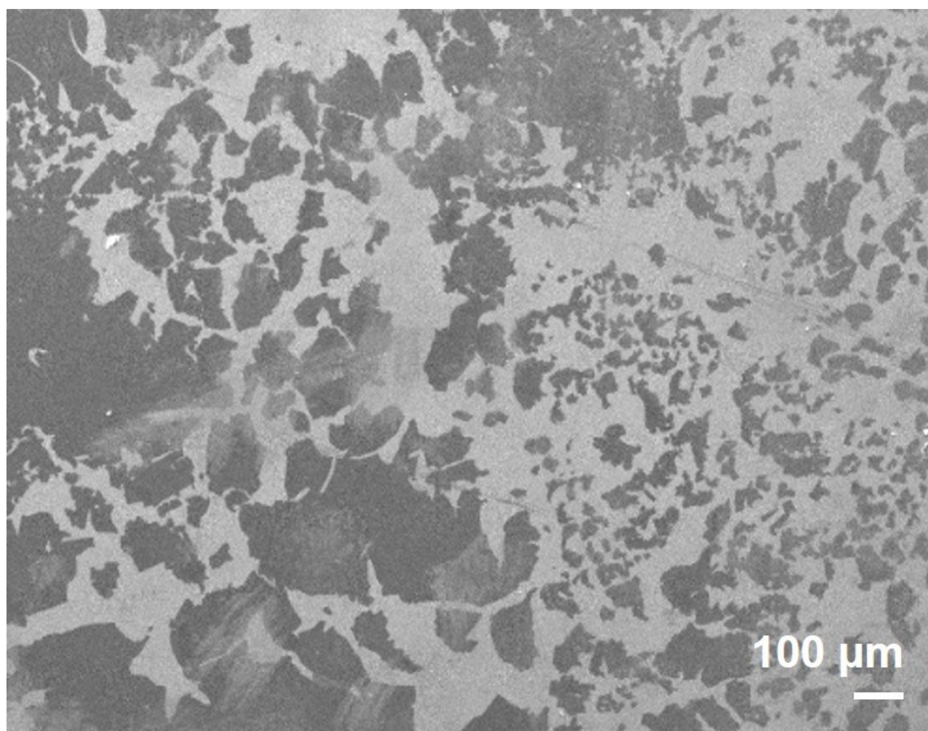

Figure S2. Top-down SEM image of GO (1L) thin film with unevenly distributed random flakes on an area scaled by a scale bar of 100 μm.

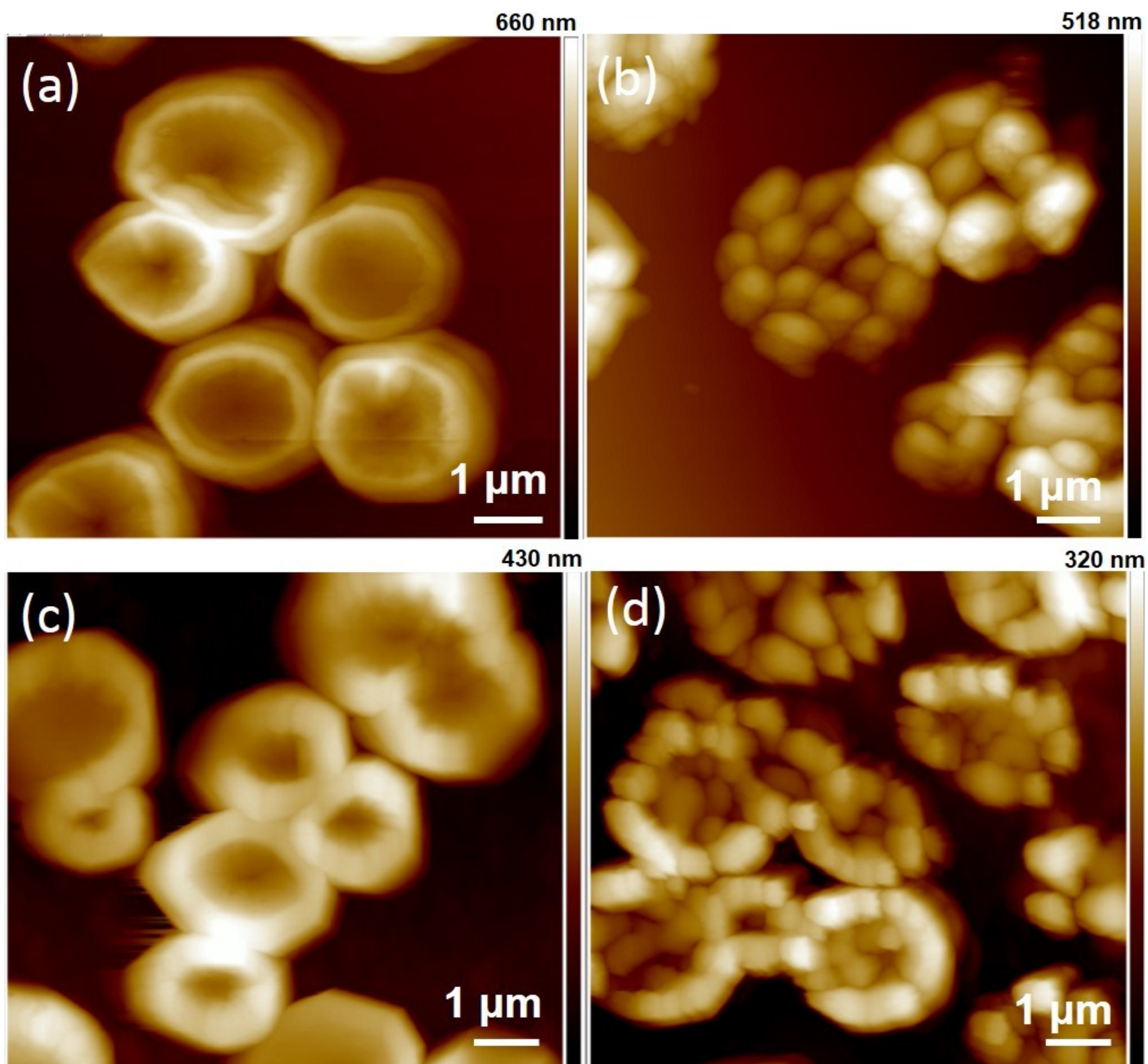

Figure S3. AFM images of a) spin casting (40 µl solution at a spin rate of 4000 rpm in 30s) of precursors (MABr and $PbBr_2$) on a Si/SiO_2 substrate at room temperature, and b) after annealing at 130°C for $MAPbBr_3$ growth, c) spin casting of MABr and $PbBr_2$ on a GO thin film at room temperature, and d) at 130°C. The numbers at the top right corner of each image indicates the height profile measured at the center on a vertical line. Scale bars are given in a 1µm scale.

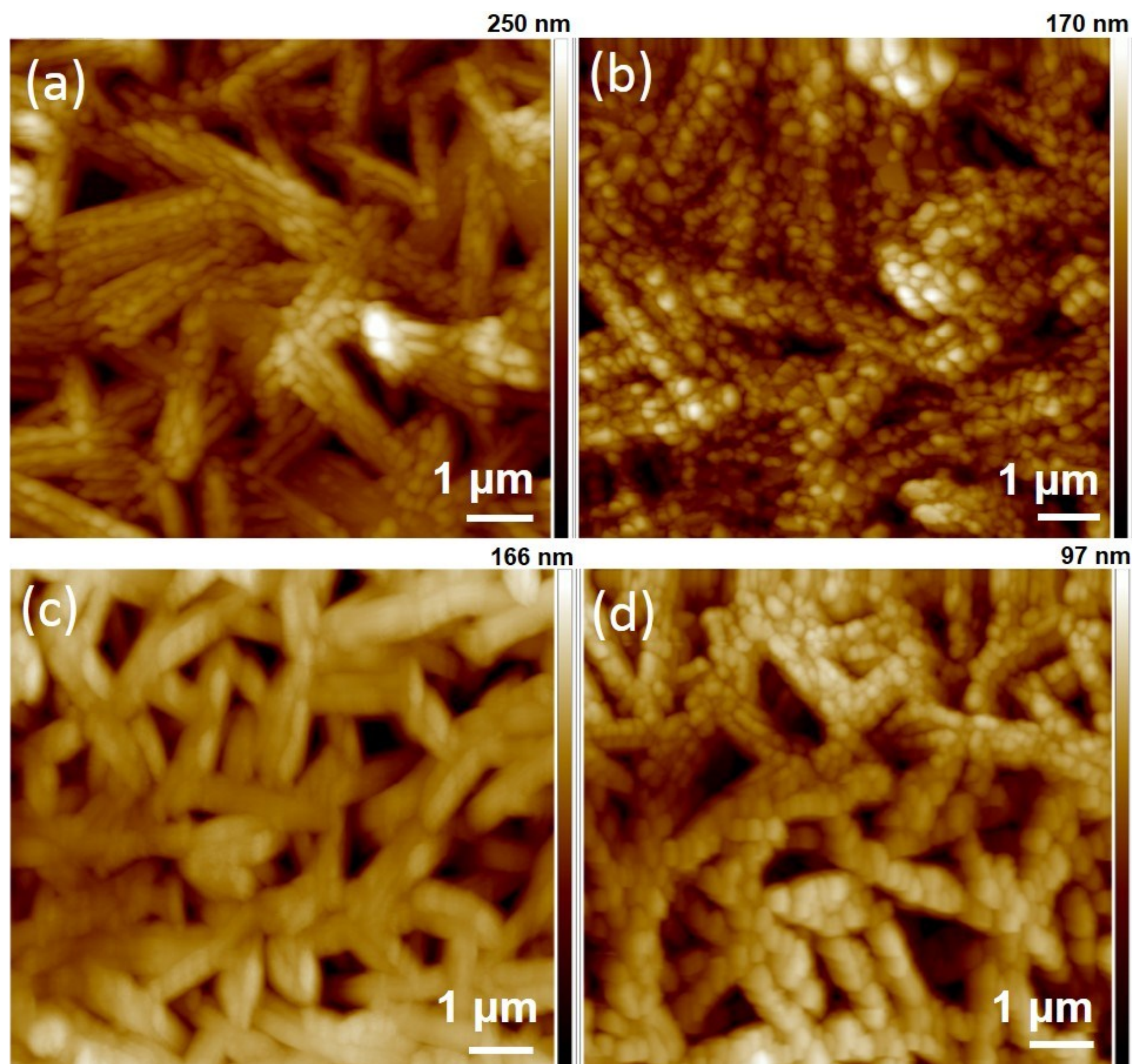

Figure S4. AFM images of a) spin casting (40 μl solution at a spin rate of 4000 rpm in 30s) of precursors (MAI and PbI_2) on a Si/SiO_2 substrate at room temperature, and b) after annealing at 130°C for $MAPbI_3$ growth, c) spin casting of MAI and PbI_2 on a GO thin film at room temperature, and d) at 130°C. The numbers at the top right corner of each image indicates the height profile measured at the center on a vertical line. Scale bars are given in a 1μm scale.

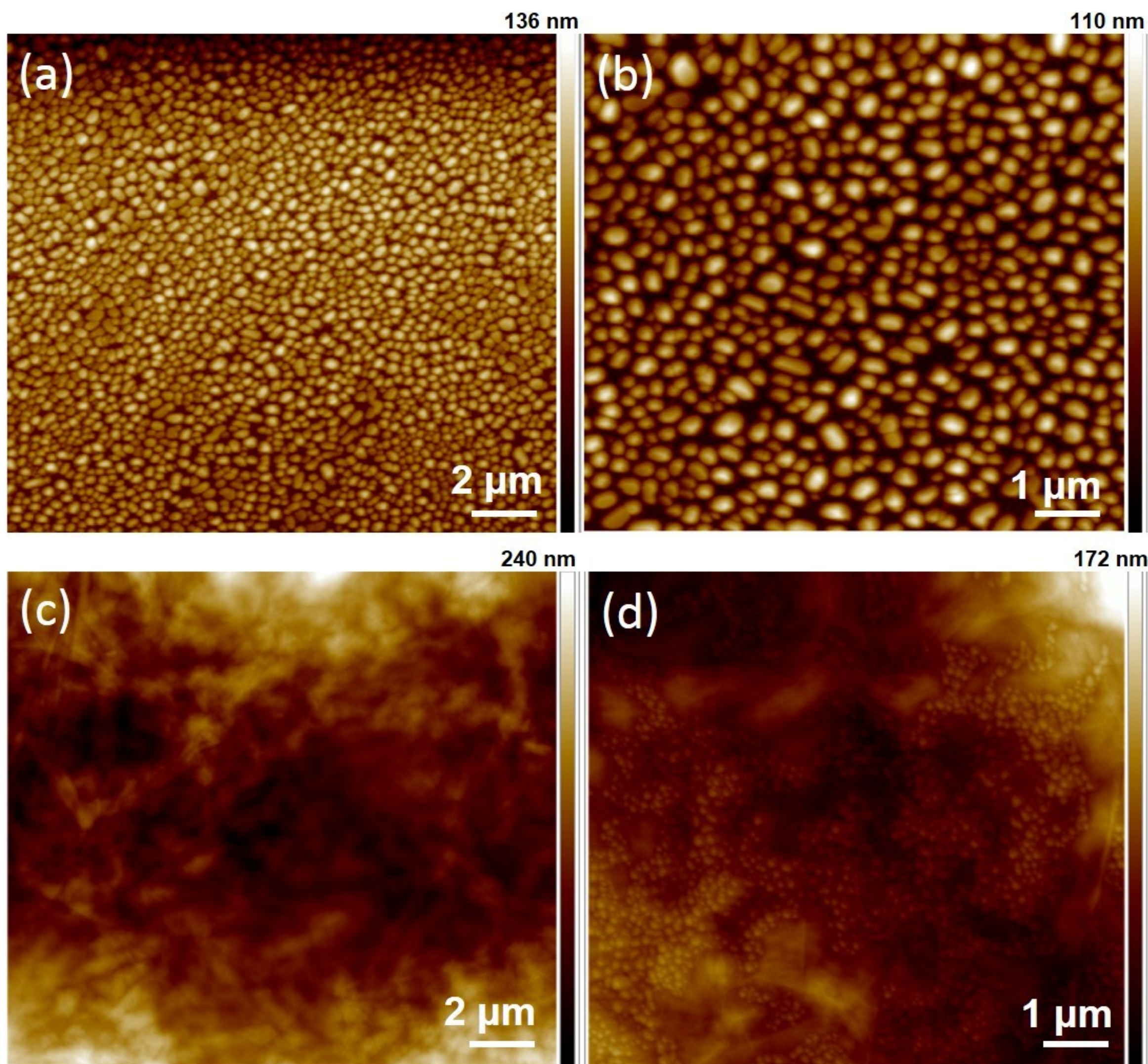

Figure S5. AFM images of a) spin casting (40 μl solution at a spin rate of 4000 rpm in 30s) of precursors (MACl and $PbCl_2$) on a Si/SiO_2 substrate at room temperature, and b) after annealing at 130°C for $MAPbCl_3$ growth, c) spin casting of MACl and $PbCl_2$ on a GO thin film for $MAPbCl_3$ growth on GO at room temperature, and d) at 130°C. The numbers at the top right corner of each image indicate the height profile measured at the center on a vertical line. Scale bars are given in a 1-2 μm scale.

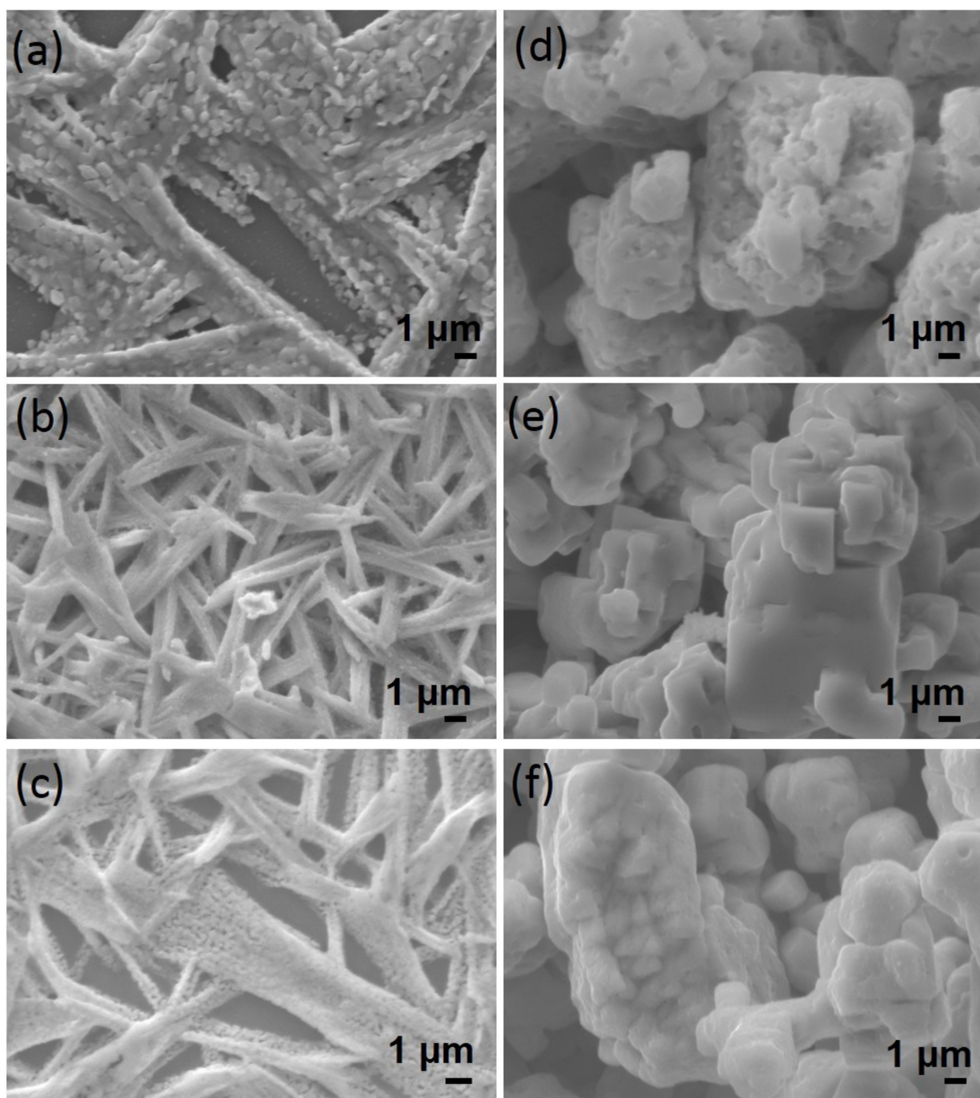

Figure S6. SEM images of $MAPbI_3$ a) after spin coating of precursors on a Si/SiO_2 substrate at 130°C, b) after of spin-coated precursors of MAI and PbI_2 on a GO (3-5 layers) thin film at room temperature, and c) after annealing at 130°C for $MAPbI_3$ growth on GO. SEM images of $MAPbCl_3$ d) after spin coating of the precursors on a Si/SiO_2 substrate at 130°C, e) spin-coated precursors of MAI and PbI_2 on a GO (3-5 layers) thin film at room temperature, and f) after annealing at 130°C for $MAPbCI_3$ growth on GO. The scale bars for each SEM image indicates 1 μm.

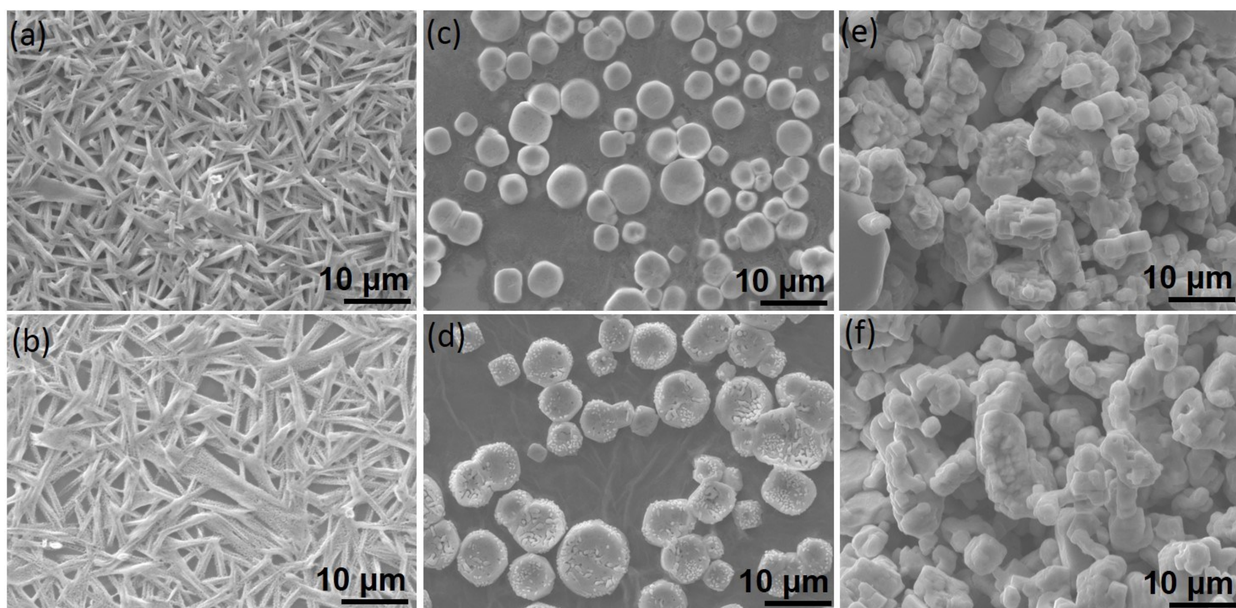

Figure S7. SEM images of $MAPbI_3$ (a-b), $MAPbBr_3$ (c-d), and $MAPbCl_3$ (e-f) crystals grown at 130°C on a) Si/SiO_2 and b) GO (3-5L), respectively. Scale bars indicate a scale of 10 µm.

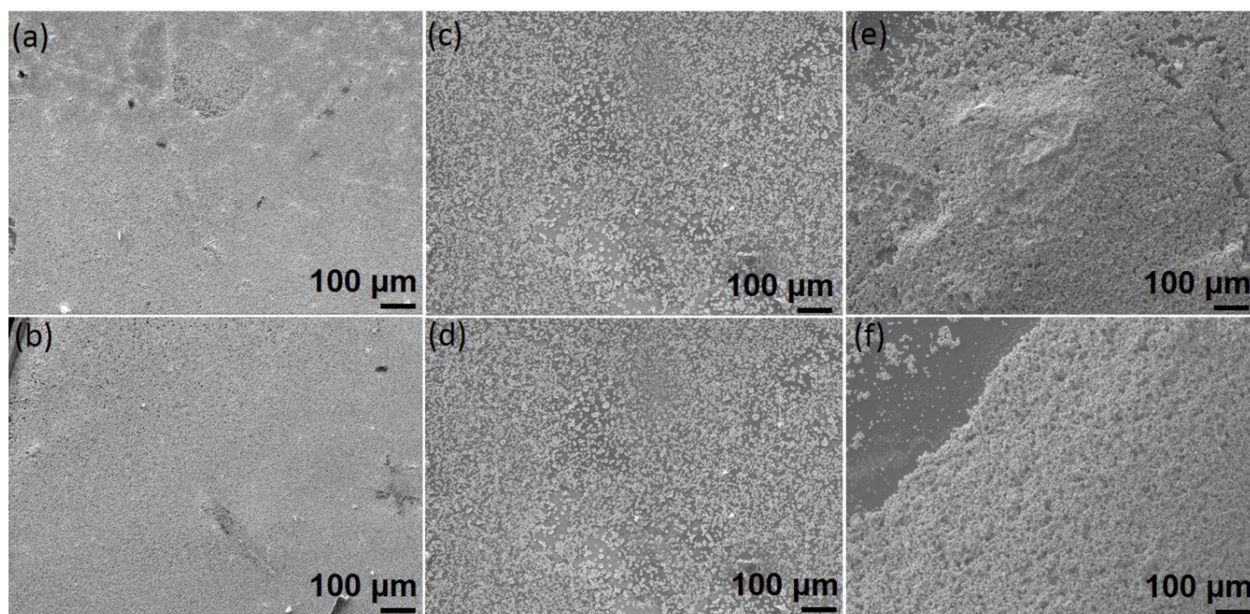

Figure S8. SEM images of $MAPbI_3$ (a-b), $MAPbBr_3$ (c-d), and $MAPbCl_3$ (e-f) crystals grown at 130°C on a) Si/SiO_2 and b) GO (3-5L), respectively. Scale bars indicate a scale of 100 µm.

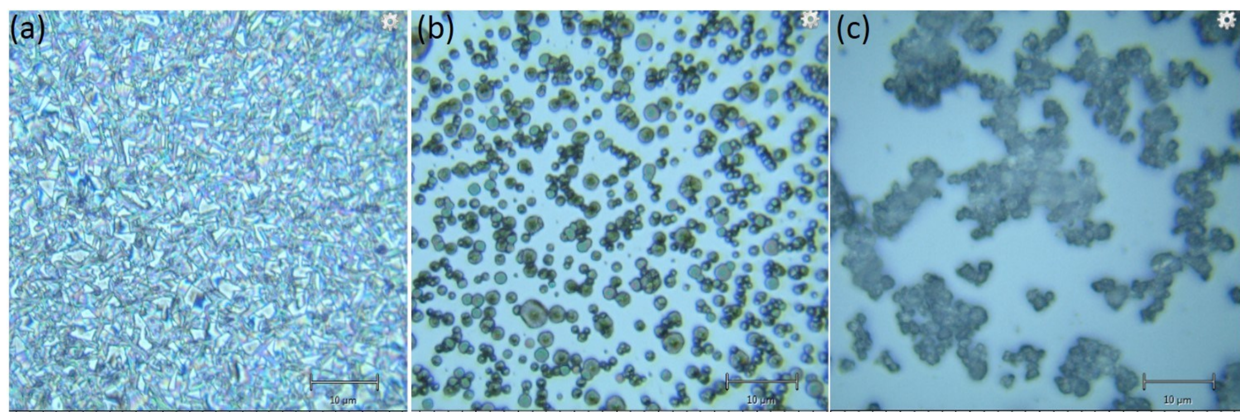

Figure S9. Optical microscope images of a) $MAPbI_3$, b) $MAPbBr_3$, and c) $MAPbCl_3$ crystals grown at 130°C on Si/SiO_2. Scale bars indicate a scale of 10 μm.

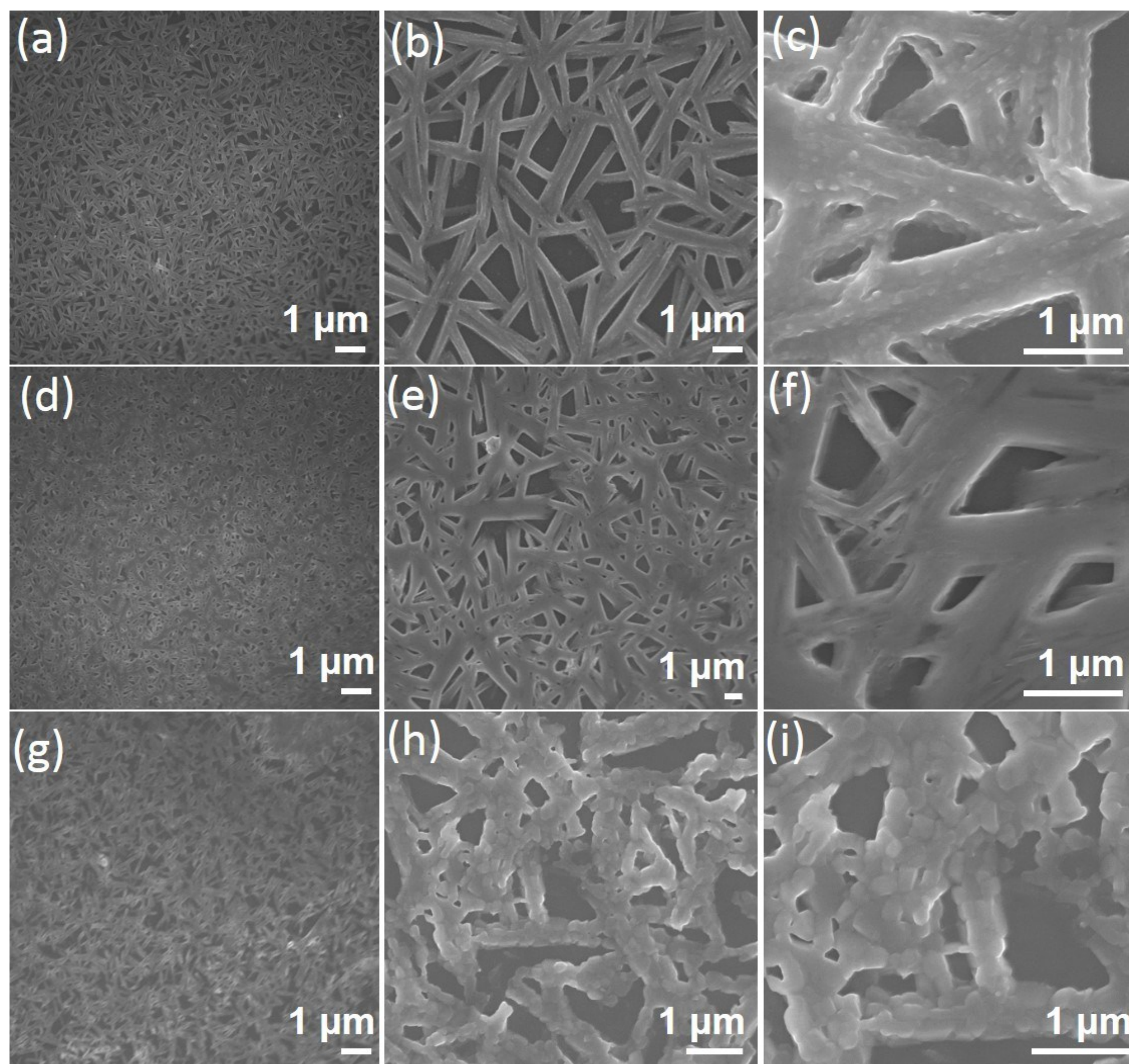

Figure S10. Top-down SEM images of $MAPbI_3$ crystals spin coated on a Si/SiO_2 from a DMF solution and further annealed for 2h (a-c), 6h (d-f), and 12h (g-i) at 60°C, as shown with images from low to high magnification (left to right).

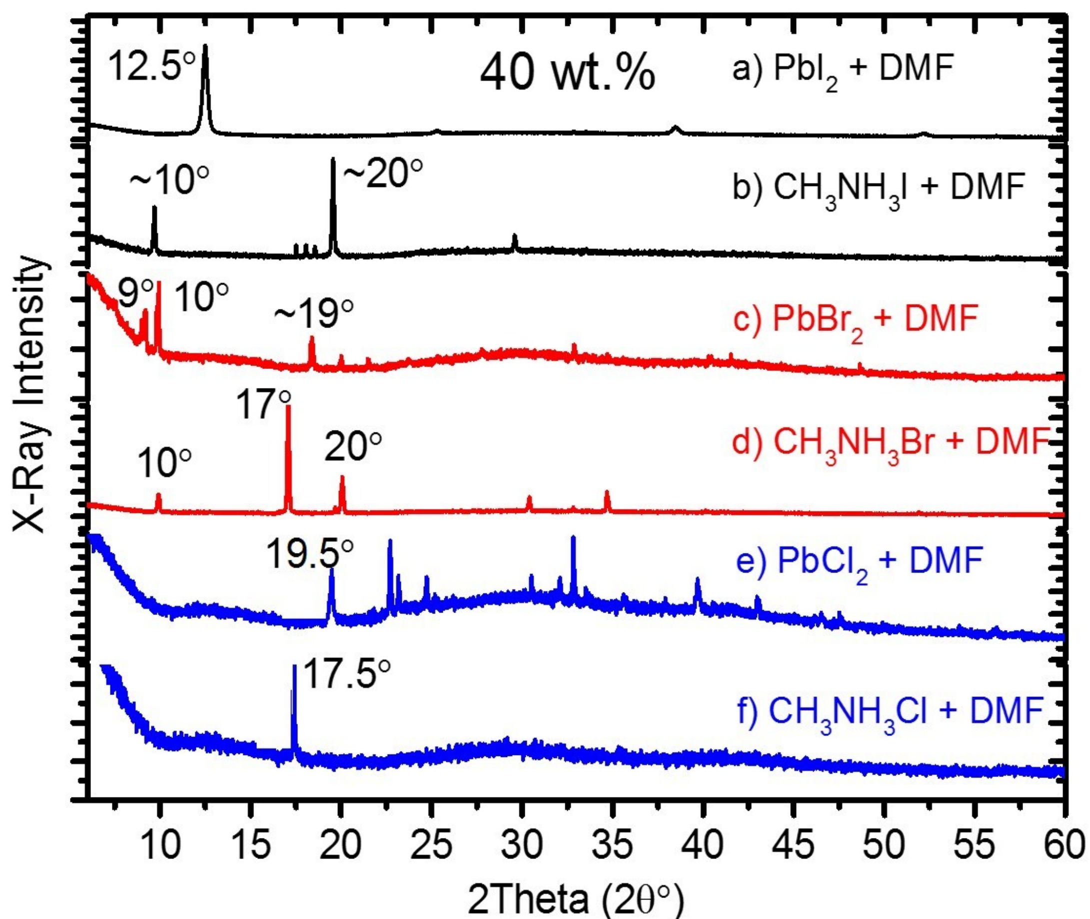

Figure S11. X-ray diffraction pattern of the precursors, namely PbI_2 (a) and CH_3NH_3I (b) spin coated in DMF (0.1g/ml) on a Si/SiO_2 substrate for $MAPbI_3$ growth. X-ray diffraction pattern of the precursors, namely $PbBr_2$ (c) and CH_3NH_3Br (d) spin coated in DMF (0.1g/ml) on a Si/SiO_2 substrate for $MAPbBr_3$ growth. X-ray diffraction pattern of the precursors, namely $PbCl_2$ (a) and CH_3NH_3Cl (b) spin coated in DMF (0.1g/ml) on a Si/SiO_2 substrate for $MAPbCl_3$ growth.

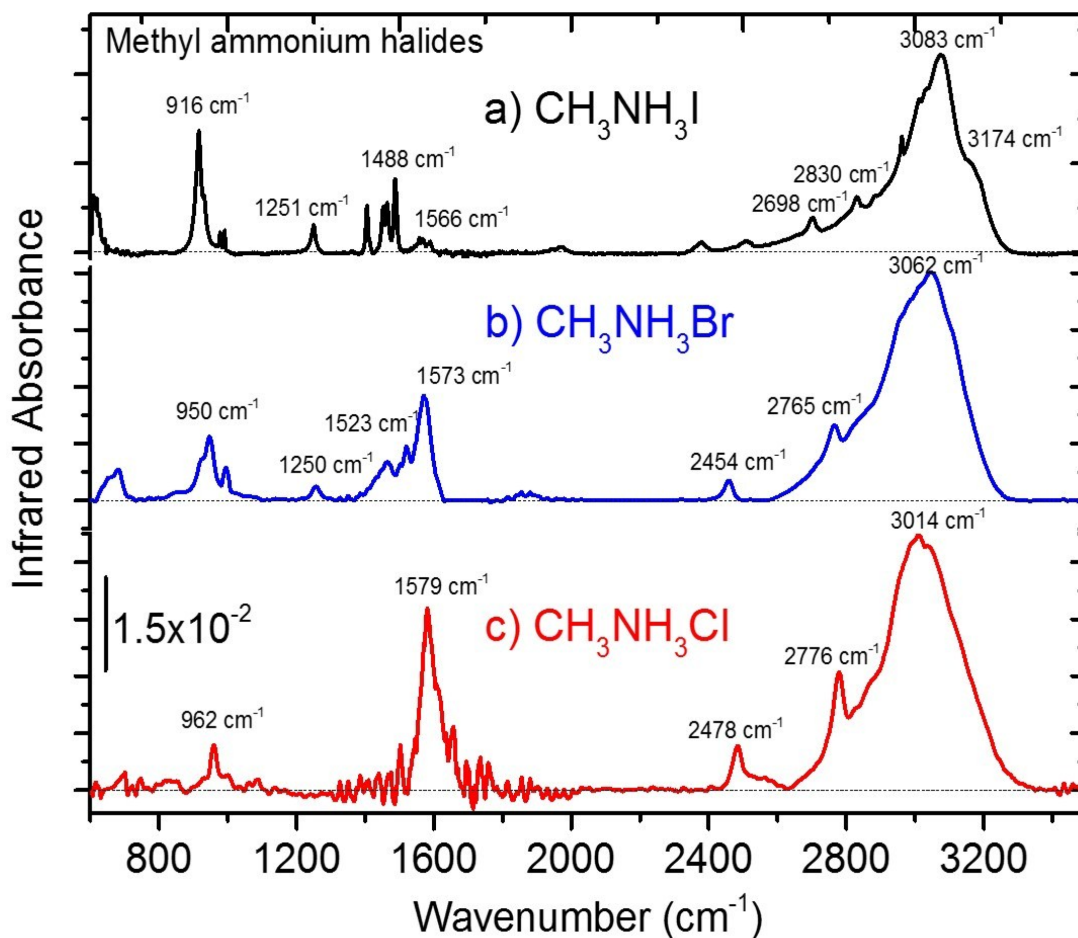

Figure S12. Infrared absorbance spectra of a) CH_3NH_3I, b) CH_3NH_3Br, and c) CH_3NH_3Cl spin coated in in DMF (0.1g/ml) on a Si/SiO_2 substrate, and referenced to infrared absorbance spectrum of a bare Si/SiO_2 for background subtraction.

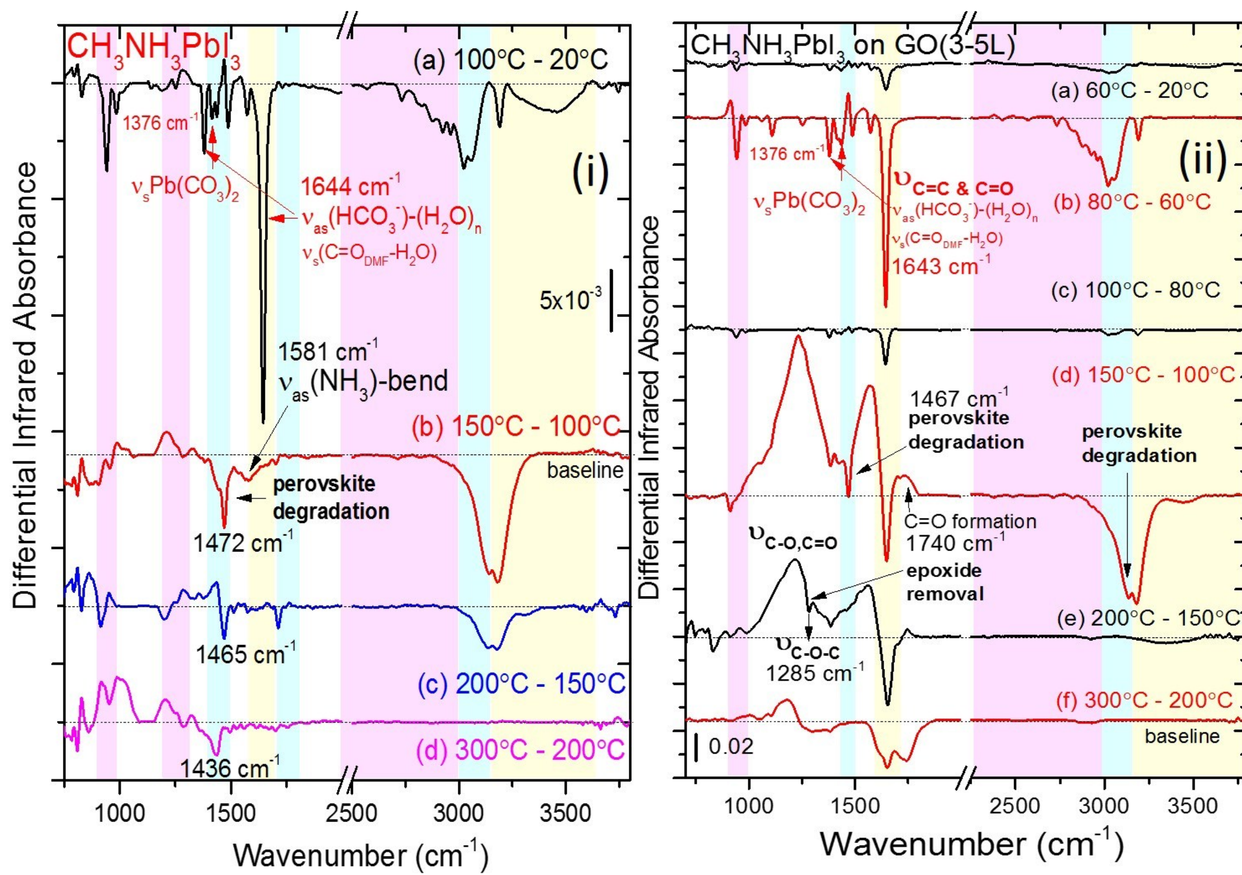

Figure S13. *In situ* differential infrared absorbance spectra of $MAPbI_3$ growth on i) Si/SiO_2 at a) 20-100°C, b) 100-150°C, c) 150-200°C, and d) 200-300°C, respectively. $MAPbI_3$ growth on ii) on a GO (3-5L) thin film at a) 20-60°C, b) 60-80°C, c) 80-100°C, d) 100-150°C, e) 150-200°C, and f) 200-300°C, respectively. Each spectrum is referenced to previous temperature to monitor the growth, and a baseline correction is applied. The baseline is given as the dotted line.

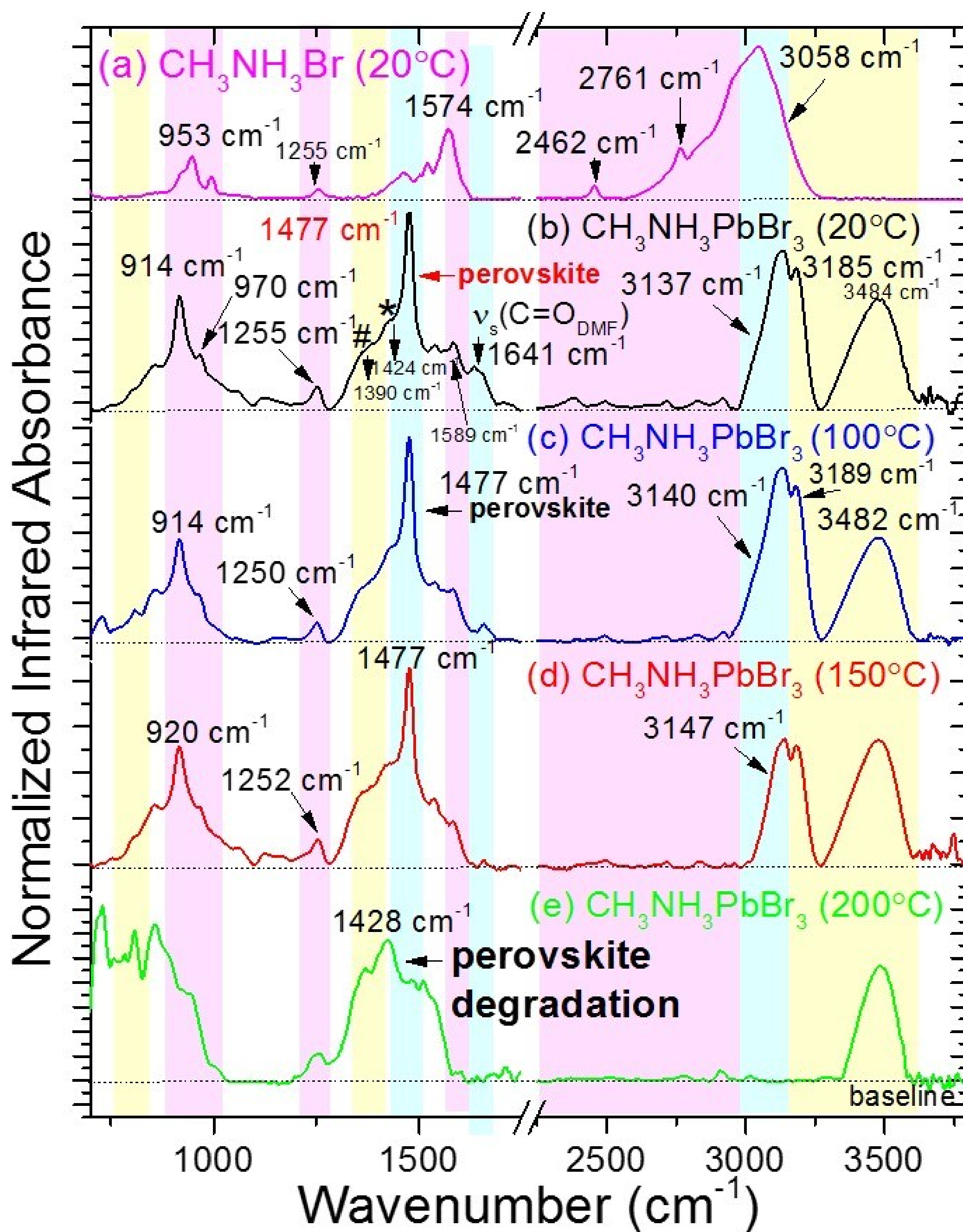

Figure S14. *In situ* transmission infrared absorbance spectra of a) spin-casted MABr from a DMF solution on a Si/SiO_2 substrate, b) spin coating of precursors (MABr and $PbBr_2$) from a 40 wt.% DMF solution on a Si/SiO_2 at room temperature (~20°C), and after annealing in argon at c) 100°C, (d) 150°C, and (e) 200°C for $MAPbBr_3$ growth on Si/SiO_2. The dotted lines indicate a baseline for each of the infrared spectrum obtained after subtracting the infrared spectrum of Si/SiO_2.

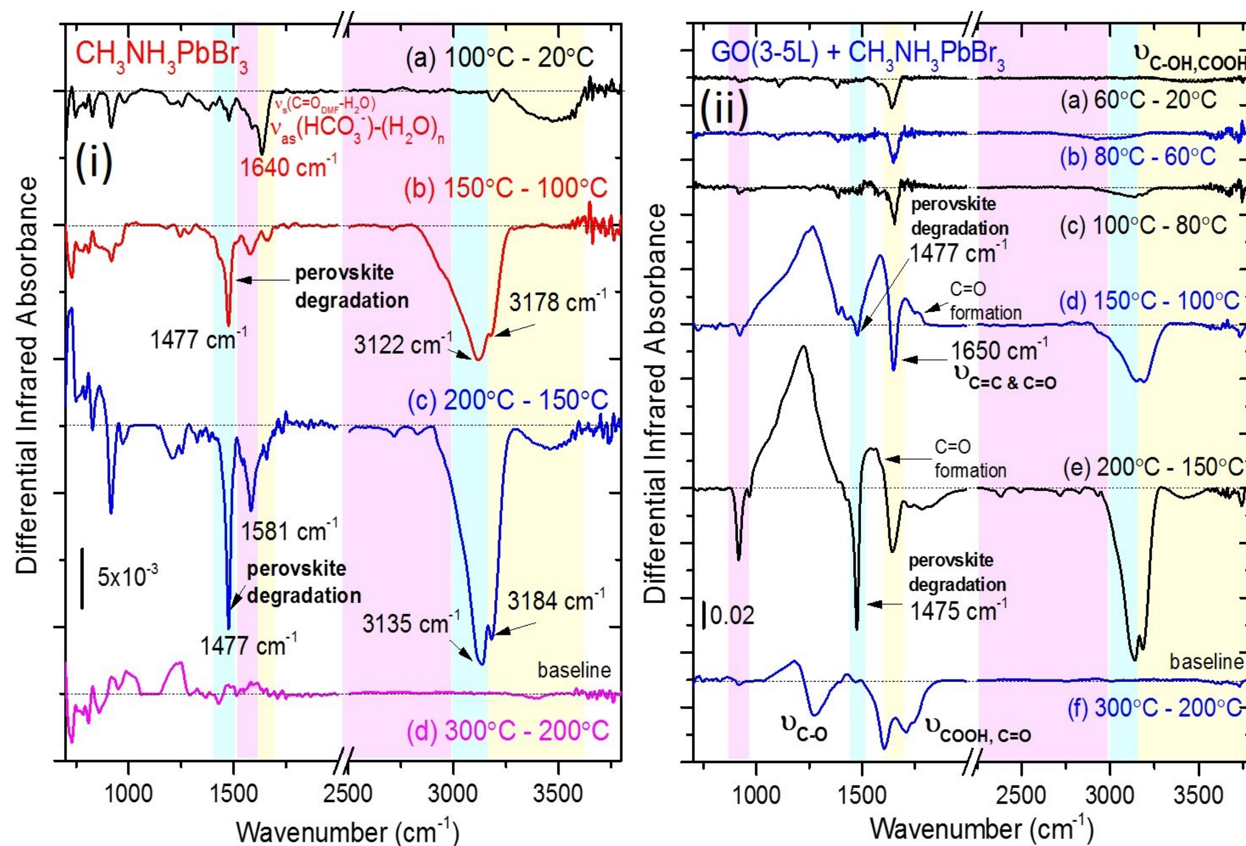

Figure S15. *In situ* differential infrared absorbance spectra of $MAPbBr_3$ growth on i) Si/SiO_2 at a) 20-100°C, b) 100-150°C, c) 150-200°C, and d) 200-300°C, respectively. $MAPbBr_3$ growth on ii) on a GO (3-5L) thin film at a) 20-60°C, b) 60-80°C, c) 80-100°C, d) 100-150°C, e) 150-200°C, and f) 200-300°C, respectively. Each spectrum is referenced to previous temperature to monitor the growth, and a baseline correction is applied. The baseline is given as the dotted line.

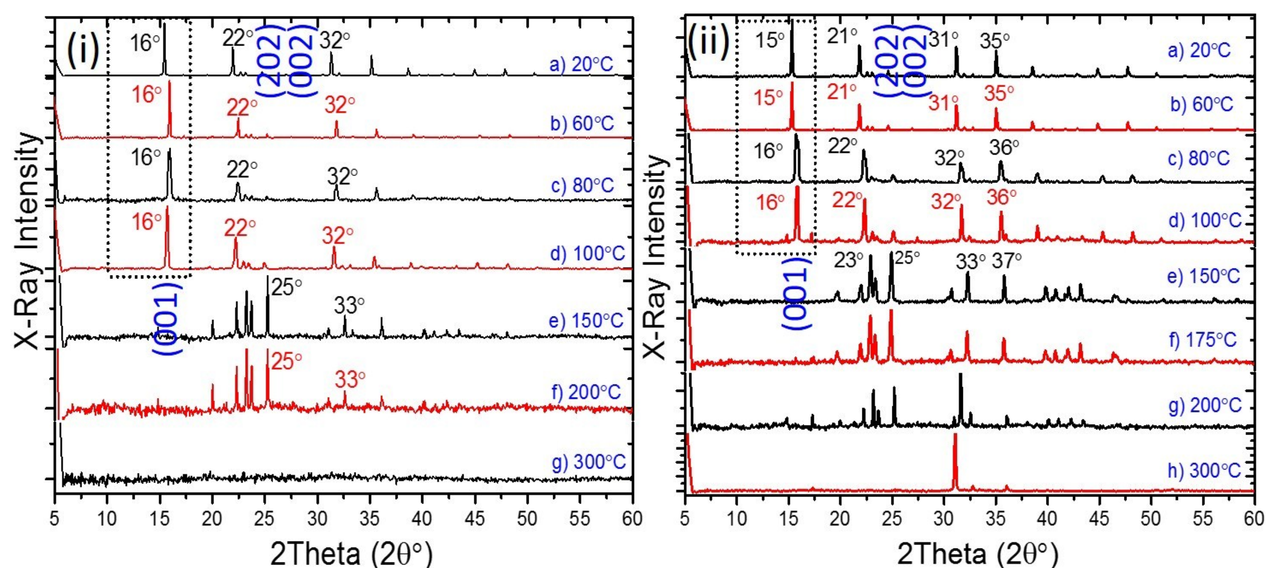

Figure S16. X-ray diffraction patterns for the growth of methylammonium lead chloride ($MAPbCl_3$) spin-coated from a 40 µl of DMF solution (i) on a Si/SiO_2 substrate at a spin rate of 4000 rpm in 30s a) at room temperature (~20°C), and further annealed on a hot plate at b) 60°C, c) 80°C, d) 100°C, e) 150°C, f) 175°C, g) 200°C, and h) 300°C for ~30 min. in a nitrogen glove box. X-ray diffraction patterns for the growth of methylammonium lead chloride ($MAPbCl_3$) spin-coated from a 40 µl of DMF solution (ii) on a Si/SiO_2 substrate at a spin rate of 4000 rpm in 30s a) at room temperature (~20°C), and further annealed on a hot plate at b) 60°C, c) 80°C, d) 100°C, e) 150°C, f) 175°C, g) 200°C, and h) 300°C for ~30 min. in a nitrogen glove box.

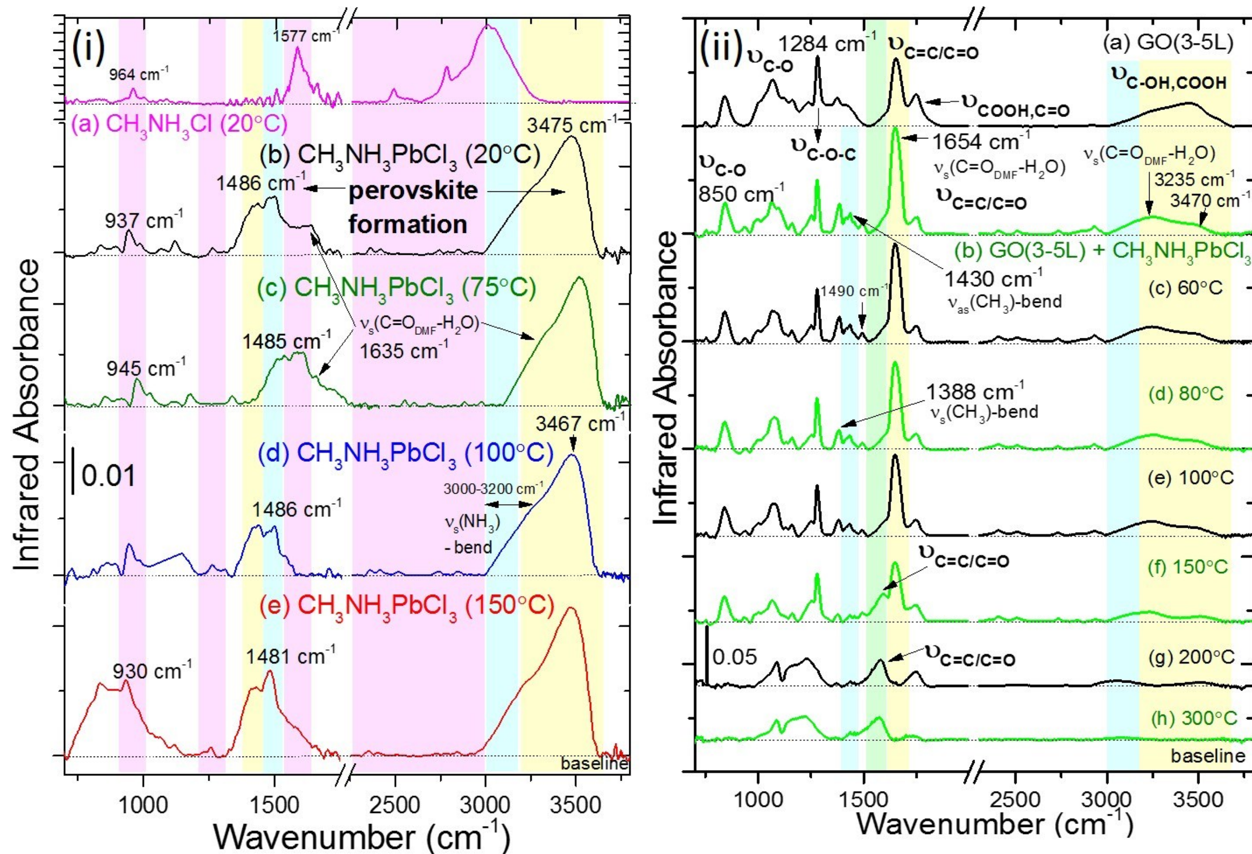

Figure S17. (i) *In situ* transmission infrared absorbance spectra of a) spin-casted MACl from a DMF solution on a Si/SiO_2 substrate as a control, b) spin coating of precursors (MACI and $PbCI_2$) from a 40 wt.% DMF solution on a Si/SiO_2 at room temperature (~20°C), and after annealing in argon at c) 75°C, (d) 100°C, and (e) 150°C for $MAPbCl_3$ growth on Si/SiO_2. (ii) *In situ* transmission infrared absorbance spectra of a) a GO thin film (3-5 layers) deposited on a Si/SiO_2 prior to any perovskite growth, b) spin coating of precursors (MACl and $PbCl_2$) from a 40 wt.% DMF solution on GO (a) at room temperature (~20°C), and after annealing in argon at c) 60°C, (d) 80°C, (e) 100°C, f) 150°C, (g) 200 °C, and (h) 300°C for $MAPbCl_3$ growth on GO.

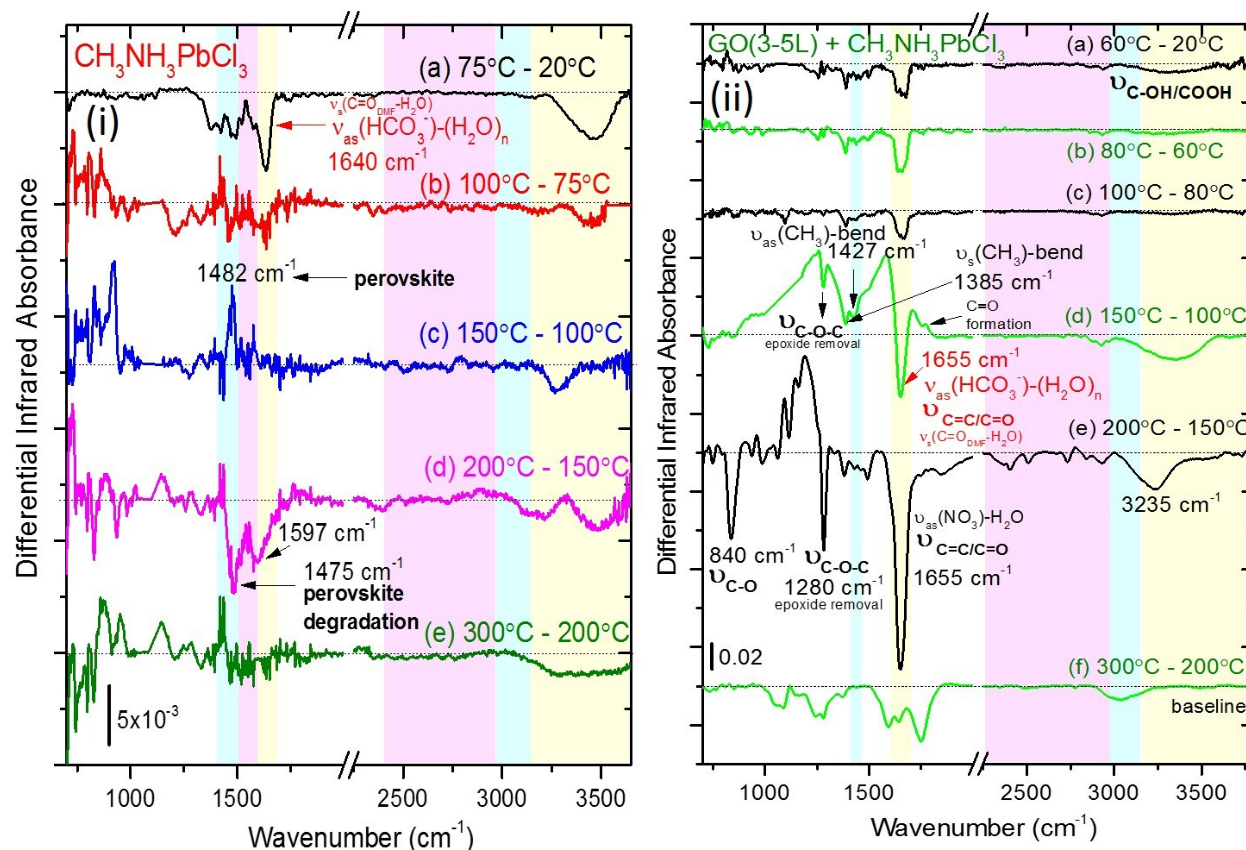

Figure S18. *In situ* differential infrared absorbance spectra of $MAPbCl_3$ growth on i) Si/SiO_2 at a) 20-75°C, b) 75-100°C, c) 100-150°C, d) 150-200°C, and e) 200-300°C, respectively. $MAPbCl_3$ growth on ii) on a GO (3-5L) thin film at a) 20-60°C, b) 60-80°C, c) 80-100°C, d) 100-150°C, e) 150-200°C, and f) 200-300°C, respectively. Each spectrum is referenced to previous temperature to monitor the growth, and a baseline correction is applied. The baseline is given as the dotted line.

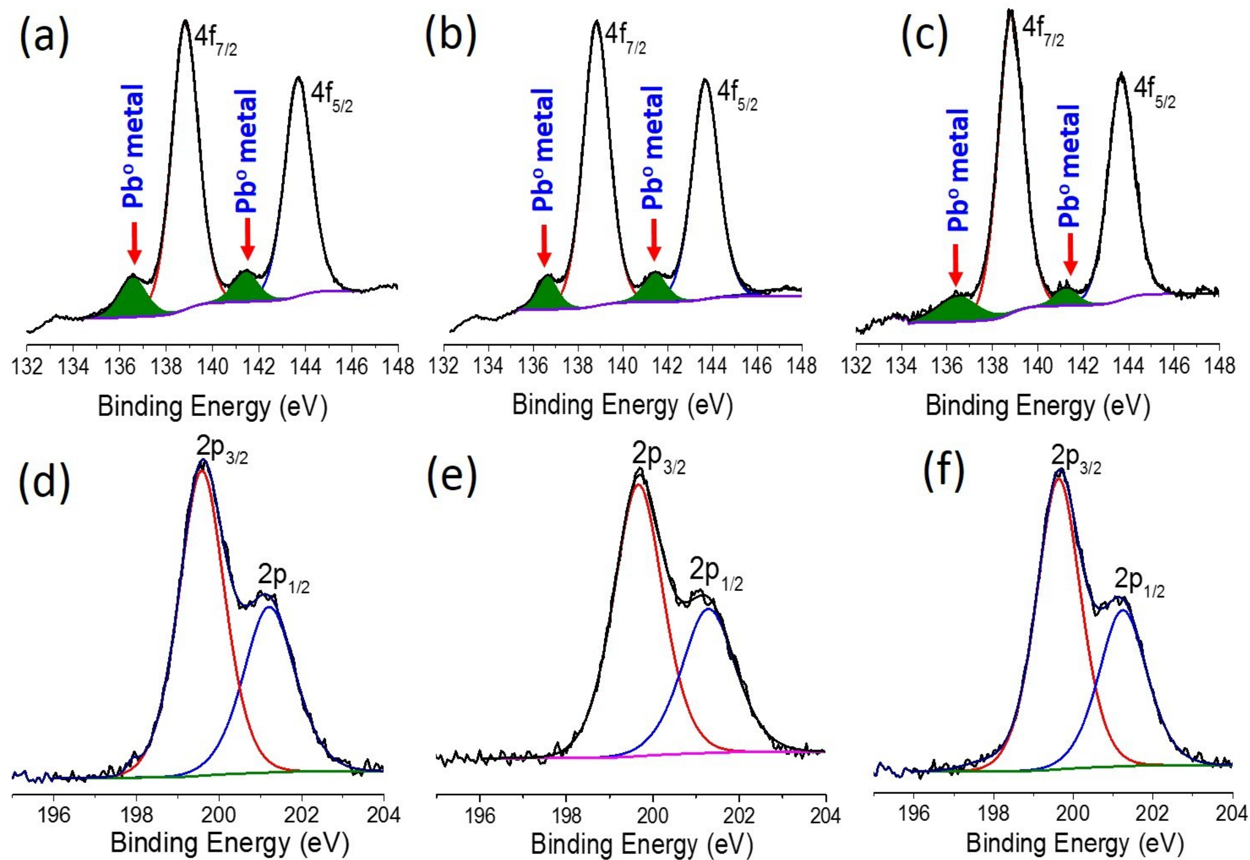

Figure S19. Pb 4f XPS spectra of spin-coated MACl and $PbCI_2$ a) on a Si/SiO_2 substrate with a further annealing at 130°C for $MAPbCI_3$ growth, and b) on a GO thin film (3-5 layers) at room temperature, c) after annealing at 130°C for $MAPbCI_3$ growth on GO indicating metallic lead (Pb^0) bands at 136.9 eV and 141.8 eV. Cl 2p XPS spectra of spin-coated MACI and $PbCI_2$ d) on a Si/SiO_2 substrate with a further annealing at 130°C for $MAPbCI_3$ growth, and e) on a GO thin film (3-5 layers) at room temperature, f) after annealing at 130°C.

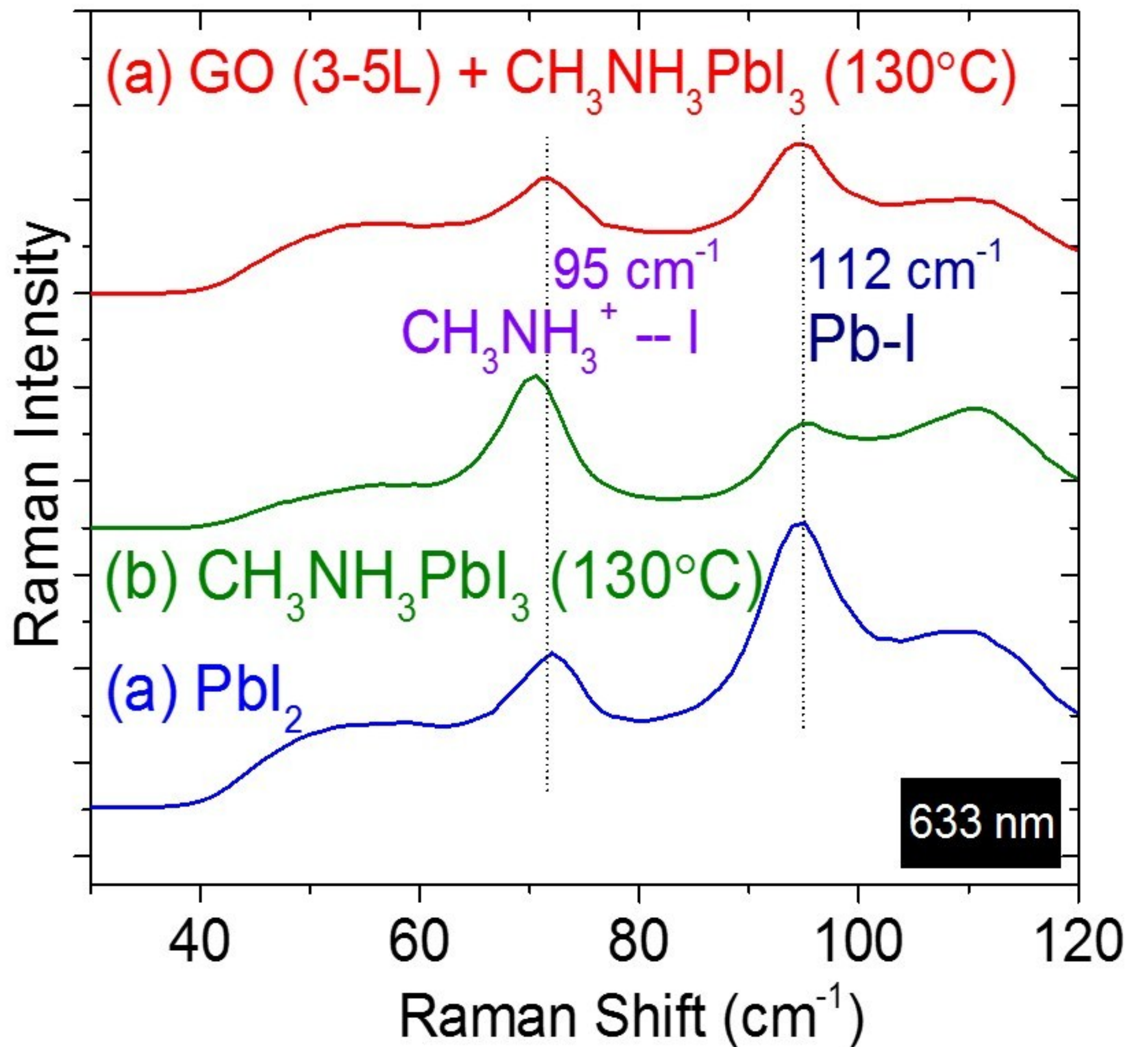

Figure S20. *In situ* micro Raman spectra of $MAPbI_3$ ($CH_3NH_3PbI_3$) grown at 130°C from a 40 wt.% of DMF solution deposited a) on a GO (3-5L) thin film and b) on a Si/SiO_2 substrate. c) Raman spectrum of PbI_2 deposited on a Si/SiO_2 from a 40 wt.% of DMF solution at room temperature. Each spectrum is collected at 633 nm laser exposure.

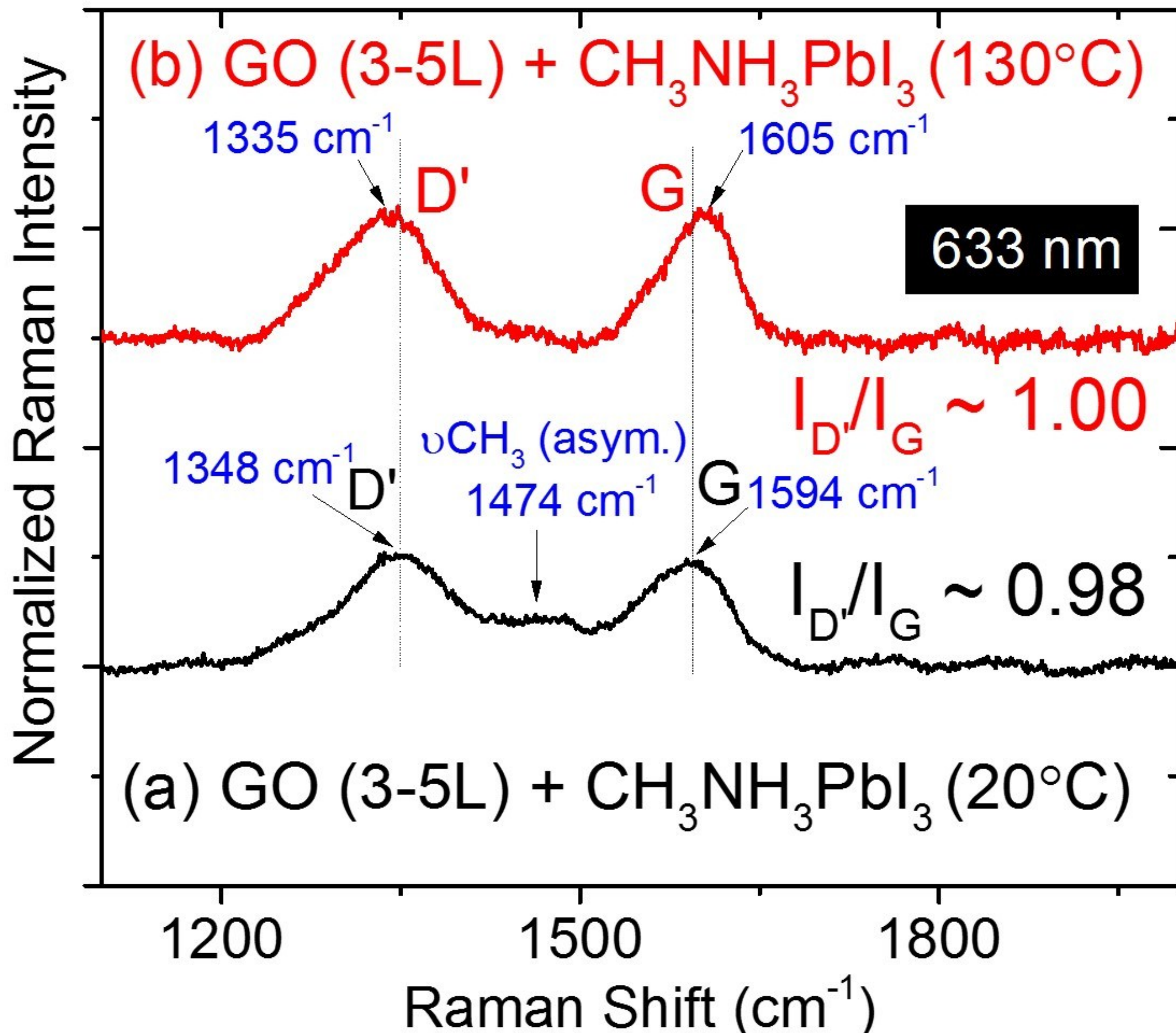

Figure S21. *In situ* micro Raman spectra of $MAPbI_3$ ($CH_3NH_3PbI_3$) grown from a 40 wt.% of DMF solution deposited on a GO (3-5L) thin film a) at 130°C (red spectrum) and b) at room temperature (black spectrum). Each spectrum is collected at 633 nm laser exposure.

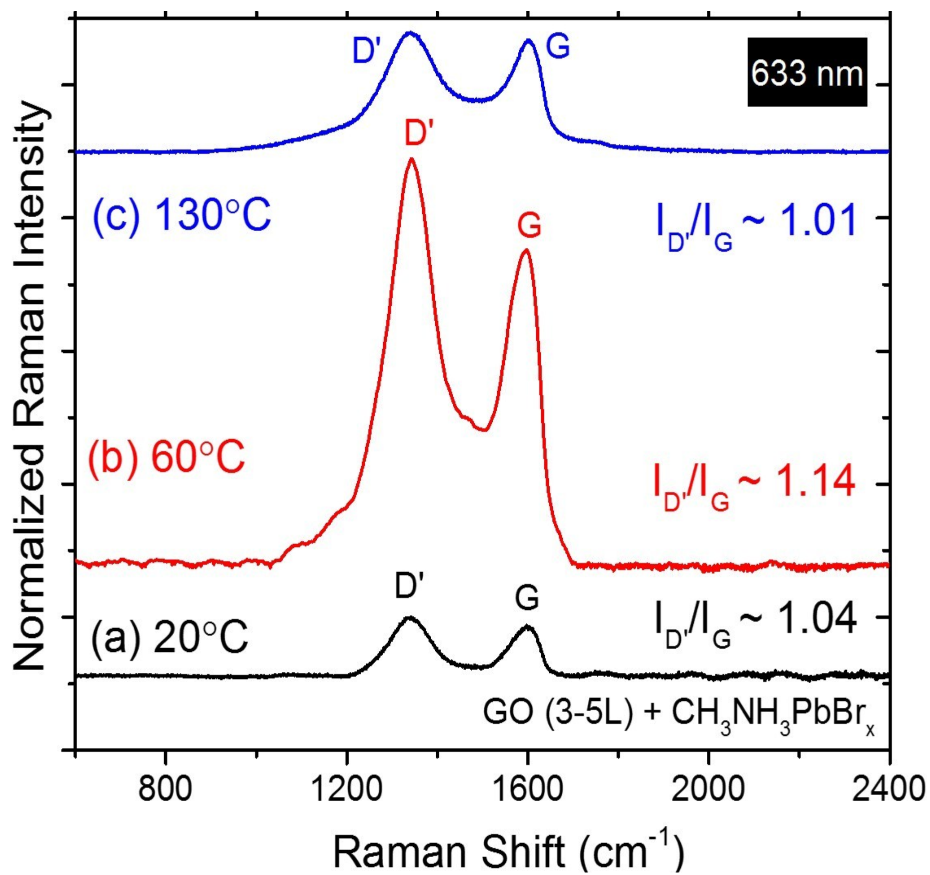

Figure S22. *In situ* micro Raman spectra of $MAPbBr_3$ ($CH_3NH_3PbBr_3$) grown from a 40 wt.% of DMF solution deposited on a GO (3-5L) thin film a) at 20°C (black spectrum), b) at 60°C (red spectrum), and c) at 130°C (blue spectrum). Each spectrum is collected at 633 nm laser exposure.

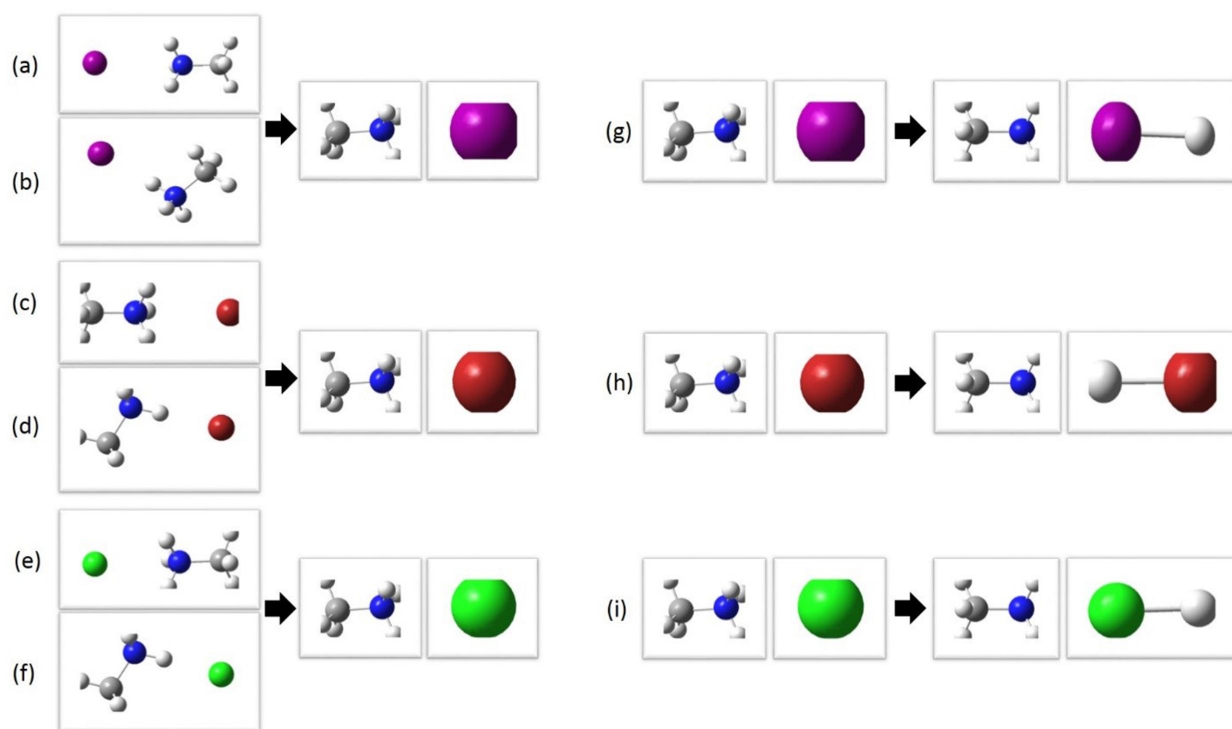

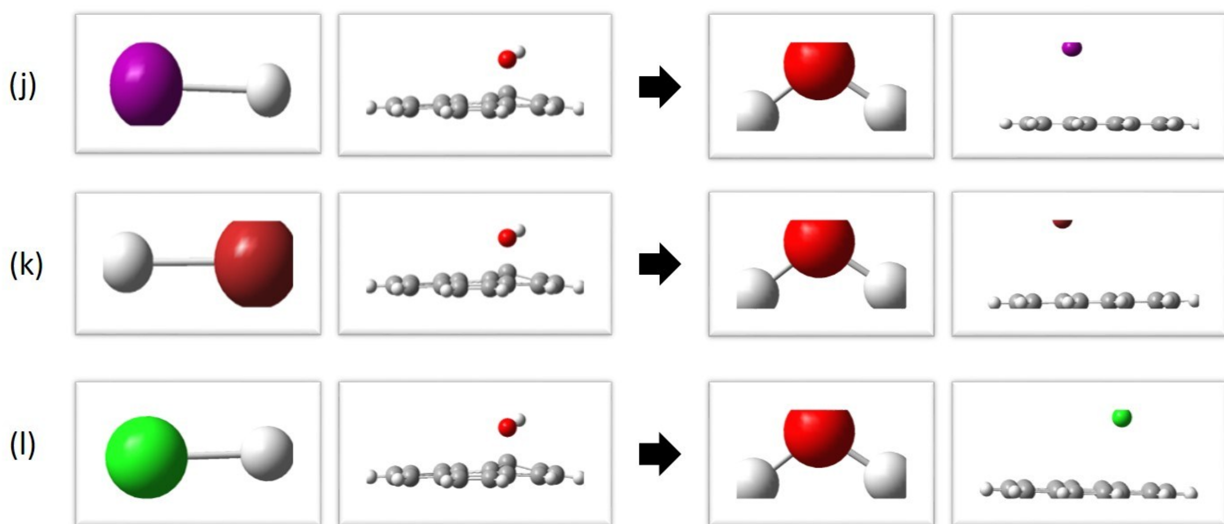

Figure S23. Atomic representation of chemical reactions for the dissociation and decomposition of the lead halide precursors given in Table 1.

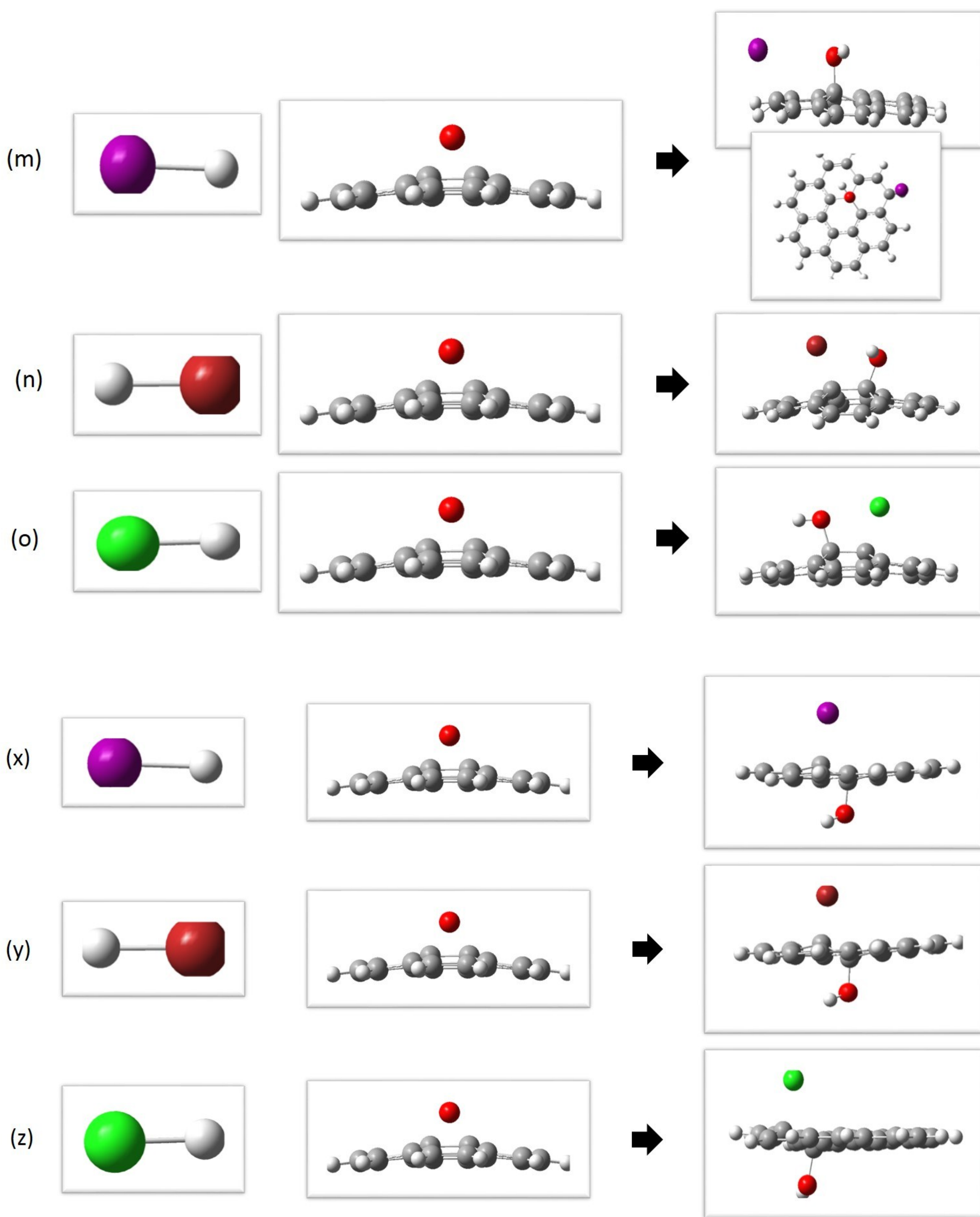

Figure S24. Atomic representation of chemical reactions for between the acid by-products and the oxygen groups of GO summarized in Table 1.

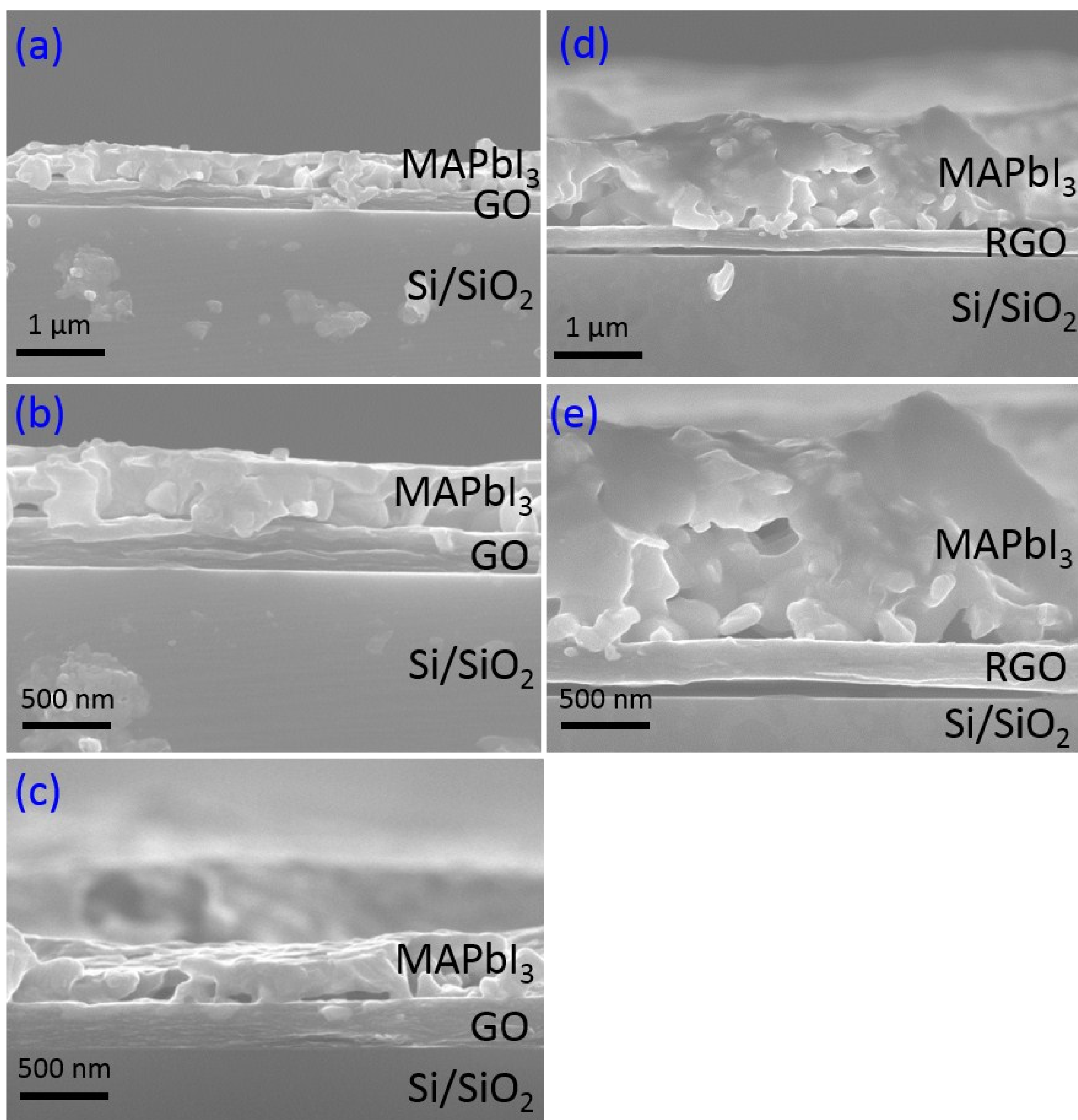

Figure S25. Cross-sectional SEM analysis of the GO/$MAPbI_3$ interface captured at the 20k (a) and 40k magnifications from different sections of the sample (b-c), and the RGO/$MAPbI_3$ interface at the 20k (d) and 40k (e) magnifications. The thickness of $MAPbI_3$ and GO/RGO is ~ 400-500 nm and ~200 nm, respectively.

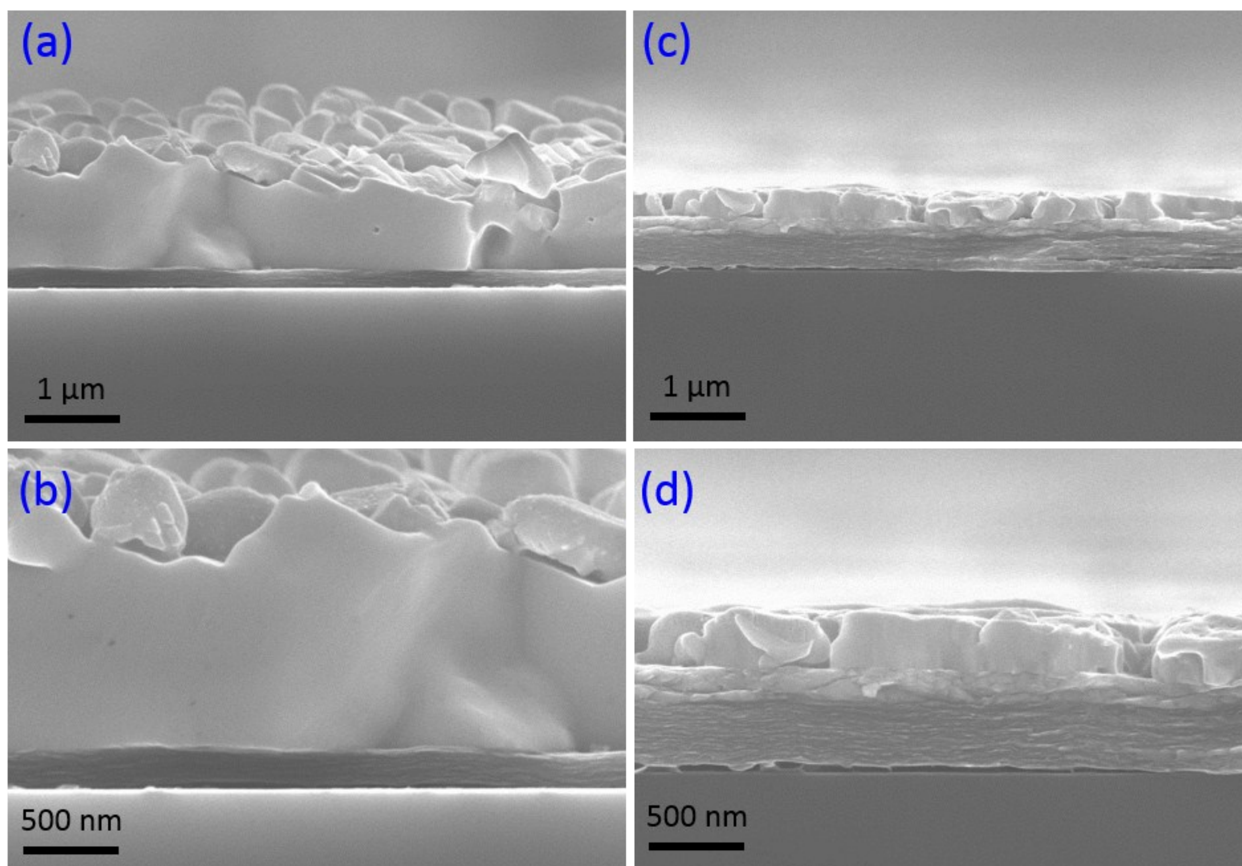

Figure S26. Cross-sectional SEM analysis of the GO/$MAPbBr_3$ interface captured at 20k (a) and 40k magnifications (b), and the RGO/$MAPbI_3$ interface at 20k (c) and 40k (f) magnifications. The thickness of $MAPbBr_3$ and GO/RGO is ~400-500 nm and ~200 nm, respectively.

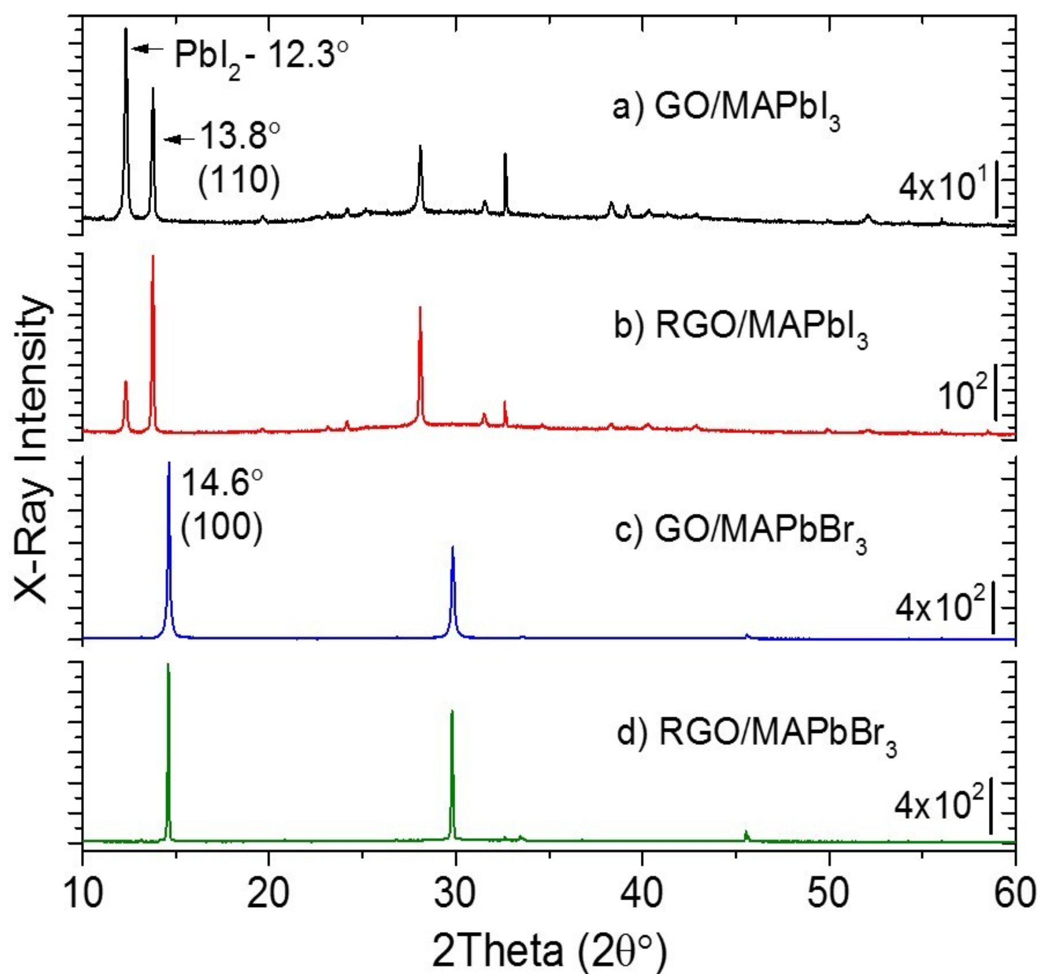

Figure S27. XRD analysis of the $MAPbI_3$ growth (130°C for 2 hours) on GO (a) and on RGO annealed at 200°C for 2 hours in nitrogen (b). XRD analysis of $MAPbBr_3$ growth (130°C for 2 hours) on GO (c), and on RGO (d). The thin films of GO and RGO are deposited on the Si/SiO_2 substrates.

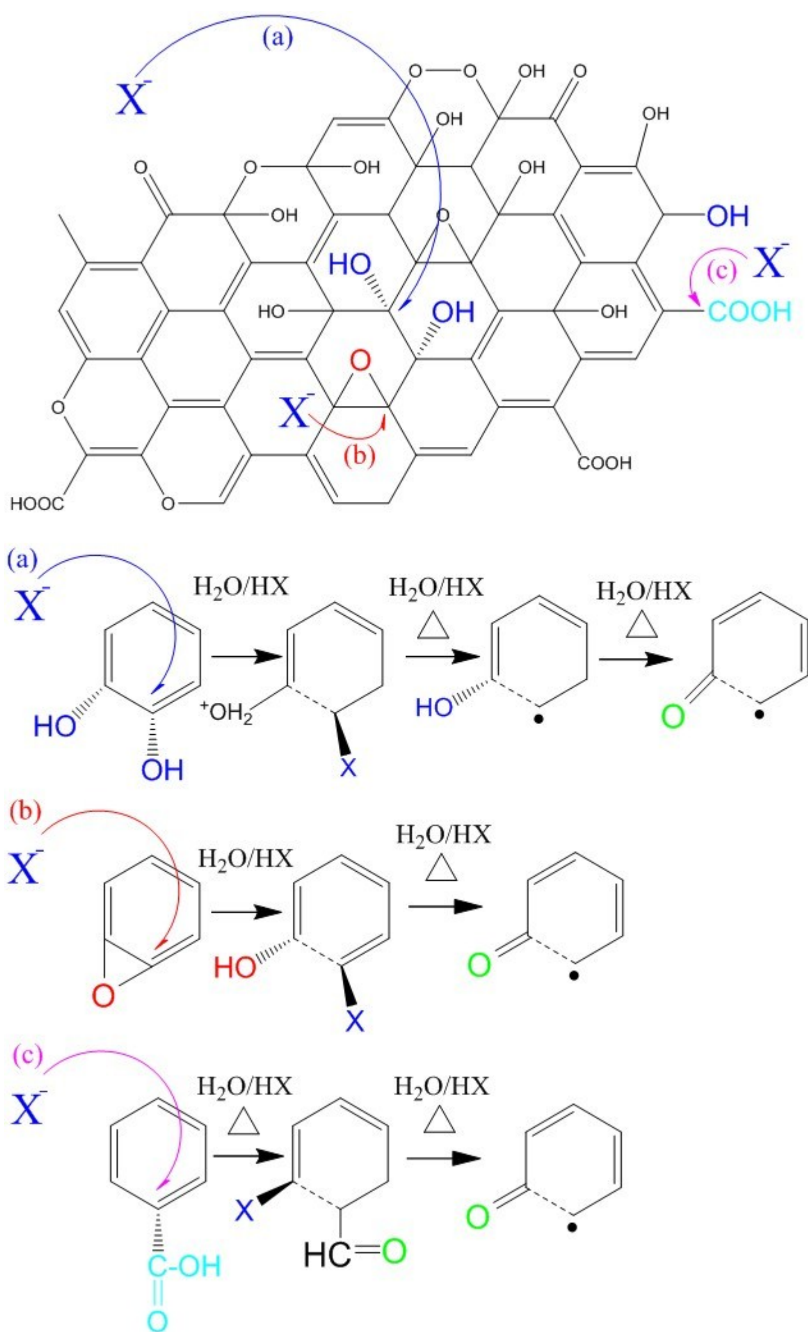

Figure S28. The proposed mechanism for the $MAPbX_3$ growth on GO for the removal of a) hydroxyls, b) epoxides, and c) carboxyls from GO. X corresponds to the halides (I, Br and Cl). The epoxides disappear for only $MAPbBr_3$ and $MAPbCl_3$ growth on GO at room temperature. Hydroxyls and carboxyls remove at elevated temperatures for $MAPbI_3$ growth on GO, which is included room temperature mechanism in (c) of $MAPbBr_3$ and $MAPbCl_3$.

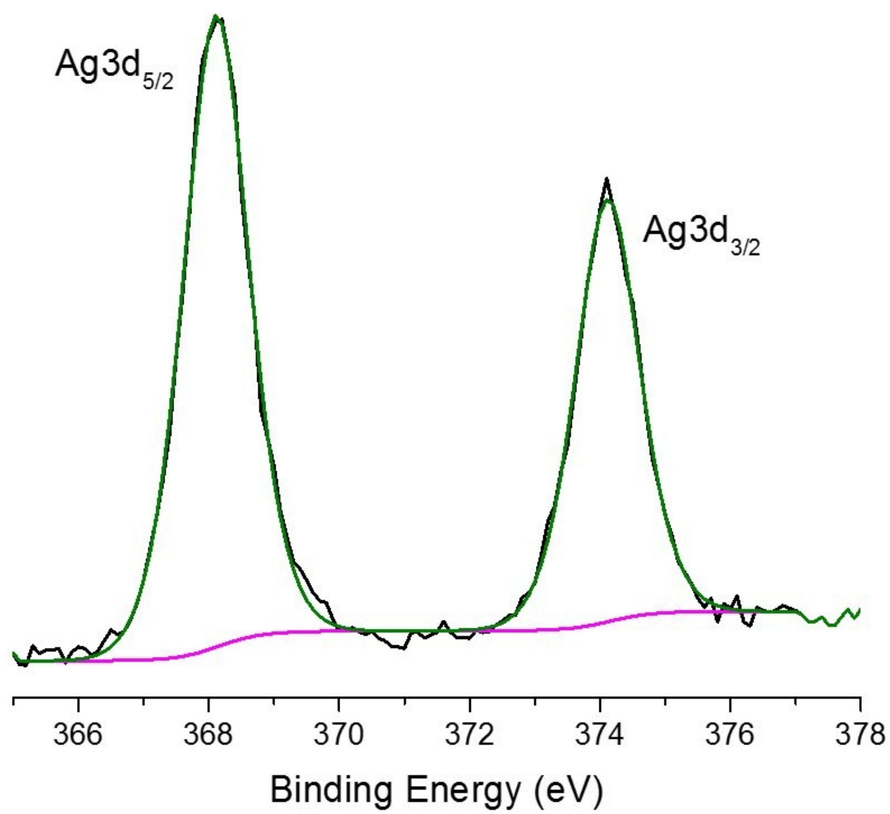

Figure S29. X-ray photoelectron spectroscopy (XPS) for Ag3d analysis for the peak calibration with the paste on the edges of the samples deposited on a Si/SiO_2 or on a GO thin film.